2020 IEEE/RSJ International Conference on Intelligent Robots and Systems (IROS)
October 25-29, 2020, Las Vegas, NV, USA (Virtual)

Gripping a Kitchen Knife on the Cutting Board

Yuechuan Xue and Yan-Bin Jia

***Abstract*— Despite more than three decades of grasping research, many tools in our everyday life still pose a serious challenge for a robotic hand to grip. The level of dexterity for such a maneuver is surprisingly "high" that its execution may require a combination of closed loop controls and finger gaits. This paper studies the task of an anthropomorphic hand driven by a robotic arm to pick up and firmly hold a kitchen knife initially resting on the cutting board. In the first phase, the hand grasps the knife's handle at two antipodal points and then pivots it about the knife's point in contact with the board to leverage the latter's support. Desired contact forces exerted by the two holding soft fingers are calculated and used for dynamic control of both the hand and the arm. In the second phase, a sequence of gaits for all the five fingers is performed quasi-statically to reach a power grasp on the knife's handle, which remains still during the period. Simulation has been performed using models of the Shadow Hand and the UR10 Arm.**

I. Introduction

Human-level dexterity has long been a grand challenge and a lofty objective to drive robotics research. One convincing evidence would be robots having the ability to manipulate tools that are used in everyday life. Preliminary progress has been made on robotic manipulation of hand tools to accomplish tasks such as drilling and pencil drawing [1], sausage pickup and bottle opening [2], bolt unscrewing with a wrench [3]. These works, carried out with visual guidance, nevertheless, did not leverage task mechanics to consider for factors such as compliance, friction, contact modes. Gripping of a kitchen knife is a highly contact-based task in which force feedback and control can be important for achieving a robust performance [4].

In this paper, we study how a pair of robotic arm and hand pick up a kitchen knife resting on the cutting board and hold its handle tightly to be ready for food cutting. We assume the hand is anthropomorphic, and the arm has at least six degrees of freedom (DOFs). Every finger of the hand is modeled as a soft finger [5], which can exert a moment about its contact. Knife gripping can be decomposed into a sequence of primitive actions such as pivoting, finger gaiting [6], caging [7], and power grasping [8], either executed quasi-statically or dynamically. An analysis of the mechanics of pivoting a block object using a parallel jaw gripper is provided in [9]. In [10], a dynamic maneuver is described to reorient a pinched object to a desired pose through wrist swing motion and grip force regulation.

Fig. 1 illustrates the start of the action. The hand first places two fingers at antipodal positions on the knife's handle. Next, leveraging the board's support as "extrinsic dexterity" [11], the hand raises the handle to let the knife pivot under gravity about the two finger contacts (Fig. 2(a)). The amount of squeeze during this lift needs to be kept at a proper level to allow the knife's rotation about the pivot and yet prevent a loss of either finger contact on the handle. The arm's movement, in the meantime, is controlled to coordinate with the knife's rotation about the pivot. The dynamics of the knife, hand, and arm are combined, while control of the arm is decoupled from that of the hand via the use of a force sensor connecting them.

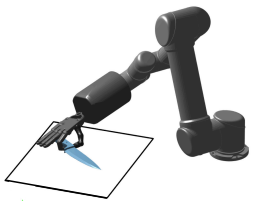

Fig. 1: Antipodal grasp.

Keeping the knife in balance with the palm involved, finger gaits and palm movements are then carried out quasi-statically on the handle to form a power grasp. This is shown in Fig. 2(b) and (c).

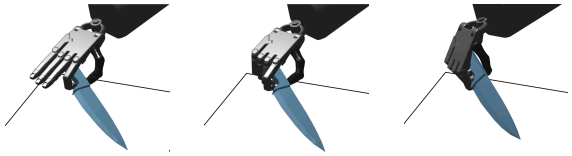

(a) Knife pivoting. (b) Finger gaiting. (c) Power grasp.

Fig. 2: Steps for gripping a resting kitchen knife.

II. Pivoting of the Knife

A kitchen knife with known geometry and mass property lies on the cutting board. The knife has a plane Π

Support for this research has been provided by the US National Science Foundation under Grant IIS-1651792. Any opinions, findings, and conclusions or recommendations expressed in this material are those of the authors and do not necessarily reflect the views of the National Science Foundation.

We would like to thank the reviewers for their valuable feedback.

The authors are with the Department of Computer Science, Iowa State University, IA, USA, yuechuan, jia@iastate.edu

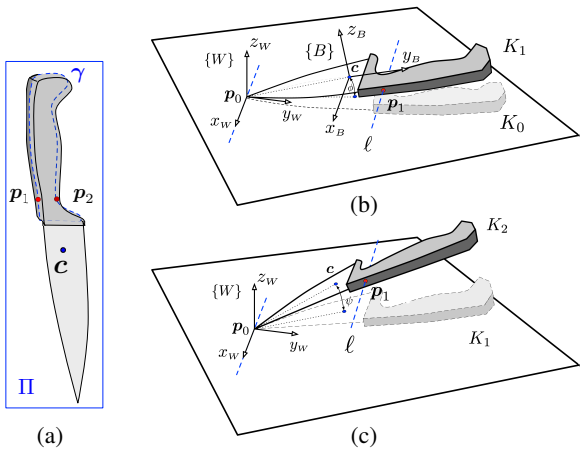

Fig. 3: (a) Kitchen knife shown with (dashed) contour intersected by its plane Π of symmetry, and two antipodal points $\boldsymbol{p}_1$ and $\boldsymbol{p}_2$ on the contour. (b) and (c) Knife's initial, intermediate, and final poses K_0, K_1, K_2 during pivoting, where K_2 results from antipodal line ℓ in K_1.

of symmetry intersecting it at a planar region bounded by a contour $\boldsymbol{\gamma}$ and containing the knife's point $\boldsymbol{p}_0$ and center $\boldsymbol{c}$ of mass.

The robotic hand will start with placing its thumb and index finger at a pair of antipodal points $\boldsymbol{p}_1$ and $\boldsymbol{p}_2$ (see Fig. 3(a)) on the handle portion of the contour $\boldsymbol{\gamma}$.[1] More specifically, the inward normals $\hat{\boldsymbol{n}}_1$ and $\hat{\boldsymbol{n}}_2$ of $\boldsymbol{\gamma}$ at $\boldsymbol{p}_1$ and $\boldsymbol{p}_2$ are opposite to each other, and collinear with the line ℓ through these two points, referred to as the *antipodal line*. Since $\boldsymbol{\gamma}$ is in the plane of symmetry, the two points must also be antipodal on the knife's handle. A body frame $\{B\}$ of the knife is located at $\boldsymbol{c}$ with its x-axis, referred to as the x_B-axis, in the direction from $\boldsymbol{p}_2$ to $\boldsymbol{p}_1$, and its x_By_B-plane coinciding with Π.

A. The Pivoting Path

A world frame $\{W\}$ is located on the cutting board at the point $\boldsymbol{p}_0$ in contact with the knife's point, as shown in Fig. 3(b). Its xy-plane is aligned with the board surface.

Denote by K_0 the knife's initial pose. Fig. 3(b) also shows an intermediate pose K_1 in which the knife's point stays at $\boldsymbol{p}_0$ but its handle is raised such that 1) its center of mass $\boldsymbol{c}$ stays in the same vertical plane as that in the pose K_0, and 2) the antipodal line ℓ is parallel to the board surface. The angle ϕ of rotation by the vector $\boldsymbol{c}-\boldsymbol{p}_0$ from its initial position is set to a small value. The x_W-axis is in the direction from $\boldsymbol{p}_2$ to $\boldsymbol{p}_1$, i.e., that of the x_B-axis in the pose K_1. Denote by $\hat{\boldsymbol{x}}, \hat{\boldsymbol{y}}$, and $\hat{\boldsymbol{z}}$ the unit vectors on the x_W-, y_W-, and z_W-axes.

[1]We refer to [12] for computation of all antipodal points on a closed plane curve.

Fig. 3(c) displays the final pose K_2 of pivoting, which results from rotating the knife in the pose K_1 about the x_W-axis until the handle's end is in contact with the palm. The angle ψ of this rotation can be calculated in advance based on the knife's geometry. Linear interpolations are used for constructing a path of the knife from K_0 to K_1 as a screw motion and another path from K_1 to K_2 as a rotation in terms of ψ. The two paths are then parameterized with time to become a single motion trajectory. The knife's position and orientation at time t are $\boldsymbol{c}(t)$ and $R(t)$, respectively. They will be used as the desired position and orientation for control purpose later on, and from now on denoted as $\boldsymbol{c}_d(t)$ and $R_d(t)$.

B. Initial Finger Placement

For convenience, we also refer to the thumb, and the index, middle, ring, and little fingers as finger 1, 2, 3, 4, 5, respectively. Finger i has joint angle vector $\boldsymbol{\theta}_i$. Its tip is modeled by a smooth curved (e.g., ellipsoidal) surface $\boldsymbol{\sigma}_i(u_i, v_i)$ in its local frame. In the world frame $\{W\}$, the surface of finger i's tip in its current pose results from a rigid transformation of $\boldsymbol{\sigma}_i(u_i, v_i)$ determined by $\boldsymbol{\theta}_i$ and $\boldsymbol{\theta}_a$, the joint angle vector of the arm. Denote the surface by $\boldsymbol{\sigma}_i[\boldsymbol{\theta}_i, \boldsymbol{\theta}_a](u_i, v_i)$.

The thumb and index finger are to be placed at $\boldsymbol{p}_1$ and $\boldsymbol{p}_2$ where their outward surface normals must coincide with the normals $\hat{\boldsymbol{n}}_1$ and $\hat{\boldsymbol{n}}_2$ on the handle, respectively. This reduces to finding the values of $\boldsymbol{\theta}_a, \boldsymbol{\theta}_i, u_i, v_i$, $i = 1, 2$ to satisfy the following ten equations:

$$\boldsymbol{\sigma}_i[\boldsymbol{\theta}_i, \boldsymbol{\theta}_a](u_i, v_i) = \boldsymbol{p}_i, \quad \hat{\boldsymbol{t}}_{ij} \cdot \left(\frac{\partial \boldsymbol{\sigma}_i}{\partial u_i} \times \frac{\partial \boldsymbol{\sigma}_i}{\partial v_i} \right) = 0,$$

where $\hat{\boldsymbol{t}}_{ij}$, $j = 1, 2$, are two orthogonal tangent vectors to $\boldsymbol{\sigma}_i$ at $\boldsymbol{p}_i$.

A subspace of solutions exists given that the total number of DOFs of the arm and two fingers far exceeds ten. To visualize one process finding a solution, we can keep the palm stationary while letting the two fingers close in until their distance reaches $\|\boldsymbol{p}_1 - \boldsymbol{p}_2\|$. The distance is achieved at the closest pair of points on different fingertips. The outward normals at these two points are colinear, which directly follows from vanishing of the partial derivatives of $\|\boldsymbol{p}_1 - \boldsymbol{p}_2\|^2$ with respect to u_1, v_1, u_2, and v_2. The arm then moves the hand until these two points and their outward normals coincide with $\boldsymbol{p}_1, \boldsymbol{p}_2$ and their inward normals, respectively.

C. Knife Dynamics

As shown in Fig. 2(a), the hand, with its thumb and index finger placed on the handle, pivots the knife around its tip $\boldsymbol{p}_0$. The tip receives a supporting force $\boldsymbol{f}_0$

from the cutting board. Negligible frictional force on the tip implies $\boldsymbol{f}_0 = f_0\hat{\boldsymbol{z}}$, for some $f_0 \geq 0$.

Let m be knife's mass and Q be its inertia tensor expressed in $\{W\}$.[2] The knife dynamics are given as

$$\sum_{i=0}^{2} \boldsymbol{f}_i + m\boldsymbol{g} = m\ddot{\boldsymbol{c}}, \tag{1}$$

where $\boldsymbol{g}$ is the gravitational acceleration. Each finger is a soft finger which exerts a moment about the contact normal with a magnitude upper-bounded by a ratio η times the normal contact force [13, p. 219]. This ratio is referred to as the torsional torque coefficient. Both fingers exert moments that achieve this ratio when the knife's handle is rotating about the antipodal line ℓ. In this situation, Euler's equation is given as

$$\sum_{i=0}^{2} \boldsymbol{r}_i \times \boldsymbol{f}_i - \eta \sum_{j=1}^{2} (\boldsymbol{f}_j^\top \hat{\boldsymbol{n}}_j)\hat{\boldsymbol{n}}_j = Q\dot{\boldsymbol{\omega}} + \boldsymbol{\omega} \times Q\boldsymbol{\omega}, \tag{2}$$

where $\boldsymbol{\omega}$ is the knife's angular velocity in $\{W\}$.

D. Desired Finger Forces for Pivoting

Let us now calculate the desired contact forces $\boldsymbol{f}_i, i = 0, 1, 2$, provided by the board and two fingers to carry out the pivoting about $\boldsymbol{p}_0$ as described in section II-A. They will be used as desired values for control shortly. Let $\boldsymbol{r}_0$ and ${}^B\boldsymbol{r}_0$ be the vector from the knife's center $\boldsymbol{c}$ of mass to its tip in frames $\{W\}$ and $\{B\}$, respectively. Hence $\boldsymbol{r}_0 = R(t)\,{}^B\boldsymbol{r}_0$. Zero motion of the tip implies $\boldsymbol{c}(t) = \boldsymbol{p}_0 - R\,{}^B\boldsymbol{r}_0$, Differentiating the previous equation and applying the identity $\dot{R}\,{}^B\boldsymbol{r}_0 = (\dot{R}R^\top)(R\boldsymbol{r}_0) = \boldsymbol{\omega} \times \boldsymbol{r}_0$, we have $\dot{\boldsymbol{c}} = -\boldsymbol{\omega} \times \boldsymbol{r}_0$ and $\ddot{\boldsymbol{c}} = -\dot{\boldsymbol{\omega}} \times \boldsymbol{r}_0 - \boldsymbol{\omega} \times \big(\boldsymbol{\omega} \times \boldsymbol{r}_0\big)$. Substituting for $\ddot{\boldsymbol{c}}$ in (1), we obtain

$$f_0\hat{\boldsymbol{z}} + \sum_{i=1}^{2} \boldsymbol{f}_i + m\boldsymbol{g} = -m\Big(\dot{\boldsymbol{\omega}} \times \boldsymbol{r}_0 + \boldsymbol{\omega} \times \big(\boldsymbol{\omega} \times \boldsymbol{r}_0\big)\Big)$$

Combine the above equation with (2):

$$\begin{bmatrix} \hat{\boldsymbol{z}} & I_{3\times3} & I_{3\times3} \\ [\boldsymbol{r}_0]_\times & [\boldsymbol{r}_1]_\times - \eta\hat{\boldsymbol{n}}_1\hat{\boldsymbol{n}}_1^\top & [\boldsymbol{r}_2]_\times - \eta\hat{\boldsymbol{n}}_2\hat{\boldsymbol{n}}_2^\top \end{bmatrix} \begin{bmatrix} f_0 \\ \boldsymbol{f}_1 \\ \boldsymbol{f}_2 \end{bmatrix} = \begin{bmatrix} -m\boldsymbol{g} - m\Big(\dot{\boldsymbol{\omega}} \times \boldsymbol{r}_0 + \boldsymbol{\omega} \times (\boldsymbol{\omega} \times \boldsymbol{r}_0)\Big) \\ Q\dot{\boldsymbol{\omega}} + \boldsymbol{\omega} \times Q\boldsymbol{\omega} \end{bmatrix}, \tag{3}$$

where $I_{3\times3}$ is the 3×3 identity matrix, and $[\boldsymbol{r}_i]_\times$ is the anti-symmetric matrix which, when multiplied with any vector, yields the cross product of $\boldsymbol{r}_i$ with that vector. The linear system (3) has a one-dimensional subspace of solutions $\begin{bmatrix} f_0 & \boldsymbol{f}_1^\top & \boldsymbol{f}_2^\top \end{bmatrix}^\top = \boldsymbol{f}^* + \lambda\hat{\boldsymbol{f}}$, where $\boldsymbol{f}^*$ is the least-square solution and $\hat{\boldsymbol{f}}$ is a vector in the null space of the 6×7 coefficient matrix.

Every solution $(f_0, \boldsymbol{f}_1, \boldsymbol{f}_2)$ is subject to three types of constraints. First, the board contact force must be positive for the knife's tip to become a pivot: $f_0 > 0$. Under this condition, the contact force generates a torque about the antipodal line ℓ, which implies that the maximum moments generated by the two soft fingers are not enough to balance the torque due to the gravitational force on the knife. Thus, the knife's handle must be rotating about ℓ, which ensures the form (2) for Euler's equation. Second, to prevent slip on the knife's handle, the finger forces $\boldsymbol{f}_1$ and $\boldsymbol{f}_2$ must stay inside their respective contact friction cones, namely, for $i = 1, 2$,

$$\boldsymbol{f}_i \cdot \hat{\boldsymbol{n}}_i > 0, \quad \|\boldsymbol{f}_i - (\boldsymbol{f}_i \cdot \hat{\boldsymbol{n}}_i)\hat{\boldsymbol{n}}_i\| < \mu|\boldsymbol{f}_i \cdot \hat{\boldsymbol{n}}_i|,$$

where μ is the coefficient of friction. If the solution set is not empty, we choose one with f_0 closest to half of the magnitude of the knife's gravitational force. Otherwise, we reparameterize the knife's pose path in section II-A with time to yield smaller angular acceleration $\dot{\boldsymbol{\omega}}$.

E. Finger and Arm Dynamics

For knife pivoting, the middle, ring, and little fingers are not used and hence not considered. Denote by $\boldsymbol{\theta}_h = (\boldsymbol{\theta}_1^\top, \boldsymbol{\theta}_2^\top)^\top$ the hand configuration. The dynamics of the thumb, index finger, and arm are combined:

$$\begin{bmatrix} \boldsymbol{\tau}_a \\ \boldsymbol{\tau}_h \end{bmatrix} = \begin{bmatrix} M_{11} & M_{12} \\ M_{21} & M_{22} \end{bmatrix} \begin{bmatrix} \ddot{\boldsymbol{\theta}}_a \\ \ddot{\boldsymbol{\theta}}_h \end{bmatrix} + \begin{bmatrix} N_1 + J_1^\top \boldsymbol{w} \\ N_2 + J_2^\top \boldsymbol{w} \end{bmatrix} \tag{4}$$

where $\boldsymbol{\tau}_a$ and $\boldsymbol{\tau}_h$ are the joint torques by the arm and hand, N_1 and N_2 includes the gravitational, centrifugal and Coriolis terms, $\boldsymbol{w} = \big(\boldsymbol{w}_1^\top, \boldsymbol{w}_2^\top\big)^\top$ stacks the external wrenches applied to the two fingers, and $(J_1, J_2) \in \mathbb{R}^{12\times(k_a+k_h')}$, with k_a and k_h' being the DOFs of the arm and the two fingers, represents the robot's Jacobian evaluated at the two contact points.

Some anthropomorphic hands are tendon driven and the joints are coupled under linear holonomic constraints $\boldsymbol{h}(\boldsymbol{\theta}_h) = \boldsymbol{0}$. In this situation, the hand dynamics need to be rewritten in terms of independent generalized coordinates $\boldsymbol{q}_h$, based on the relationship $\dot{\boldsymbol{\theta}}_h = V\dot{\boldsymbol{q}}_h$, for some matrix V. In the rest of the paper, we will use $\boldsymbol{q}_a = \boldsymbol{\theta}_a$ and $\boldsymbol{q}_h$ to denote the robot configuration.

Left multiplying $M_{21}M_{11}^{-1}$ to the first row of (4) and then subtracting it from the second row, we obtain the hand dynamics in the following form:

$$\boldsymbol{\tau}_h = M_h\ddot{\boldsymbol{q}}_h + N_h + J_h^\top \boldsymbol{w}, \tag{5}$$

where $M_h = V^\top\big(M_{22} - M_{21}M_{11}^{-1}M_{12}\big)V$, $N_h = V^\top\big(N_2 - M_{21}M_{11}^{-1}N_1 + M_{21}M_{11}^{-1}\boldsymbol{\tau}_a\big)$, and $J_h =$

[2] $Q = R_k Q_k R_k^\top$, where Q_k is the diagonalized inertia tensor in the frame defined by the knife's principal axes, and R_k is the matrix describing the rotation of this frame from $\{W\}$.

$V^\top \big(J_2 - J_1 M_{11}^{-1} M_{12}\big)$. The hand dynamics (5) contain the arm's state (joint angles $\boldsymbol{q}_a$ and velocities $\dot{\boldsymbol{q}}_a$) as well as its torques $\boldsymbol{\tau}_a$ due to a coupling between the arm and hand. The arm's joint accelerations $\ddot{\boldsymbol{q}}_a$ have been eliminated, which means we can have the full hand dynamics once knowing the arm and hand's states and the former's joint torques $\boldsymbol{\tau}_a$.

F. Arm Trajectory and Control

To the arm, the hand can be treated as an external workload measurable by a force/torque sensor mounted between the arm's end-effector and the hand. With the sensor reading $\boldsymbol{w}_s \in \mathbb{R}^6$, the arm's dynamics become

$$\boldsymbol{\tau}_a = M_a \ddot{\boldsymbol{q}}_a + N_a(\boldsymbol{q}_a, \dot{\boldsymbol{q}}_a) + J_s^\top \boldsymbol{f}_s, \tag{6}$$

where M_a is the arm's mass matrix, N_a includes the nonlinear terms, and J_s is the arm's Jacobian matrix at the reference point of the sensor.

The arm is responsible for moving the palm along its desired trajectory to realize pivoting performed by the thumb and index finger. Denote by $\boldsymbol{x}_a \in \mathbb{R}^6$ the pose of the arm's end-effector as determined by its location $\boldsymbol{p}_a$ and orientation matrix R_a,[3] where

$$\boldsymbol{p}_a(t) = \begin{cases} R(t)R(0)^\top \boldsymbol{p}_a(0), & t \in [0, t_1], \\ \boldsymbol{p}_a(t_1) + \boldsymbol{p}_1(t) - \boldsymbol{p}_1(t_1) & t \in (t_1, t_2], \end{cases}$$

$$R_a(t) = \begin{cases} R(t)R(0)^\top R_a(0), & t \in [0, t_1], \\ R_a(t_1), & t \in (t_1, t_2]. \end{cases}$$

The desired trajectory $\boldsymbol{x}_{a,d}$ of the arm can be constructed eventually from that of the knife.

Let J_a be the Jacobian matrix of the arm for $\boldsymbol{x}_a$. We have $\dot{\boldsymbol{x}}_a = J_a \dot{\boldsymbol{q}}_a$ and $\ddot{\boldsymbol{x}}_a = \dot{J}_a \dot{\boldsymbol{q}}_a + J_a \ddot{\boldsymbol{q}}_a$. Assuming that the arm is not at a singular configuration, we obtain $\ddot{\boldsymbol{q}}_a = J_a^\dagger(\ddot{\boldsymbol{x}}_a - \dot{J}_a \dot{\boldsymbol{q}}_a)$, where $J_a^\dagger$ is the Penrose-Moore inverse of J_a. To control the arm, we make use of the error $\boldsymbol{x}_{a,e} = \boldsymbol{x}_{a,d} - \boldsymbol{x}_a$. From the arm dynamics (6), a task space position controller is then employed as follows:

$$\boldsymbol{\tau}_{a,\mathrm{ctrl}} = M_a J_a^\dagger \Big(\alpha - \dot{J}_a \dot{\boldsymbol{q}}_a\Big) + N_a + J_s^\top \boldsymbol{f}_s,$$

where $\alpha = \ddot{\boldsymbol{x}}_{a,d} + K_{a,d}\dot{\boldsymbol{x}}_{a,e} + K_{a,p}\boldsymbol{x}_{a,e} + K_{a,i}\int \boldsymbol{x}_{a,e}\mathrm{d}t$, and $K_{a,d}, K_{a,p}, K_{a,i}$ are the damping, proportional and integral gains, respectively.

G. Finger Control

The knife's desired trajectory $(c_d(t), R_d(t))$ is determined in section II-A. For $i = 1, 2$, at time t along the trajectory there is a desired contact frame $\{F_{id}\}$ on the tip of finger i that is located at $\boldsymbol{p}_i$ as determined from $(c_d(t), R_d(t))$ with its z-axis aligned with the contact normal $\hat{\boldsymbol{n}}_i$ and y-axis parallel to $R_d(t)^\top \hat{\boldsymbol{z}}$.

The actual trajectory of $\boldsymbol{p}_i$ is described by

$$\boldsymbol{p}_i(t) = R(t)\big({}^B\boldsymbol{r}_i - {}^B\boldsymbol{r}_0\big), \quad t \in [0, t_2],\ i = 1, 2,$$

during the pivoting action, where ${}^B\boldsymbol{r}_i$ is the vector from $\boldsymbol{c}$ to $\boldsymbol{p}_i$ in the knife's body frame. The actual contact frame on the fingertip $\{F_i\}$ coincides with the desired frame $\{F_{id}\}$ at $t = 0$.

In order to let the knife track the desired pivoting trajectory, the forces exerted by the fingers should be exactly the same as obtained from section II-D. Instead of controlling all the contact forces directly, we let the index finger follow its desired trajectory under position control, and the thumb apply the desired normal contact force while following the trajectory in other dimensions. When all the contacts with the knife are maintained with no slip, it can be verified from the dynamics that its translational and rotational accelerations will stay the same as their desired values. In a sense, the normal contact force by the thumb determines the other two contact forces by the index finger and the board.

At time t along the real knife trajectory, we let $\boldsymbol{x}_i(t) \in \mathrm{SE}(3)$ represent the transformation from the desired contact frame $\{F_{id}\}$ to the actual contact frame $\{F_i\}$. Since finger i has $k_i < 6$ degrees of freedom, its configuration can be uniquely determined by a subset $\boldsymbol{s}_i = (\boldsymbol{s}_{iv}^\top, \boldsymbol{s}_{if}^\top)$ of coordinates in $\boldsymbol{x}_i(t)$, where position and force control are applied on $\boldsymbol{s}_{iv}$ and $\boldsymbol{s}_{if}$, respectively. We introduce a $k_i \times 6$ selection matrix $S_i = (S_{iv}^\top, S_{if}^\top)^\top$ such that $\boldsymbol{s}_{iv} = S_{iv}\boldsymbol{x}_i$ and $\boldsymbol{s}_{if} = S_{if}\boldsymbol{x}_i$.

The index finger is subject to position control only, thus, $\boldsymbol{s}_2 = \boldsymbol{s}_{2v}$. The thumb has the z-component of $\boldsymbol{x}_1(t)$ selected for force control while the other $k_1 - 1$ for position control. Note that the directions for its motion control and force control are orthogonal to each other, which leads to $(0, 0, 1, 0, 0, 0) S_{1v}^\top = 0$. By setting a large enough gain for the index finger, we may assume that this finger and the knife's handle together constitute a hard environment for the thumb to be in contact with. Consequently, the position along the z-direction of the task frame $\{P_i\}$ is fixed and $\boldsymbol{s}_{1f} = 0$ always holds. In fact, $\boldsymbol{s}_1$ is now completely determined by $\boldsymbol{s}_{1v}$ as a result of $\boldsymbol{s}_1 = S_1 S_{1v}^\top \boldsymbol{s}_{1v}$.

Let $\boldsymbol{q}_i$ be the independent generalized coordinates of the i-th finger. For $i = 1, 2$, $\dot{\boldsymbol{s}}_i = H_i \dot{\boldsymbol{q}}_i$, where $H_i = S_i T_i J_{c,i}$, where T_i transforms linear and angular velocities from the world frame $\{W\}$ to the change rate of $\boldsymbol{x}_i$ in the task frame $\{P_i\}$, and $J_{c,i}$ is the finger Jacobian evaluated at the contact point $\boldsymbol{p}_i$. The $k_i \times k_i$ matrix H_i is invertible if the finger joints are not in a singular configuration. Differentiation of $\dot{\boldsymbol{s}}_i = H_i \dot{\boldsymbol{q}}_i$

[3] We explicitly represent $\boldsymbol{x}_a$ by the coordinates of $\boldsymbol{p}_a$ and three Euler angles.

yields, for $i = 1, 2$, $\ddot{\boldsymbol{s}}_i = \dot{H}_i \dot{\boldsymbol{q}}_i + H_i \ddot{\boldsymbol{q}}_i$, from which we obtain $\ddot{\boldsymbol{q}}_i = H_i^{-1}\big(\ddot{\boldsymbol{s}}_i - \dot{H}_i \dot{\boldsymbol{q}}_i\big)$. From the last equation and (5), the hand controller can be described as

$$\boldsymbol{\tau}_{h,\mathrm{ctrl}} = M_h \begin{bmatrix} H_1^{-1}\Big(S_1 S_{1v}^\top \alpha_1 - \dot{H}_1 \dot{\boldsymbol{q}}_1\Big) \\ H_2^{-1}\Big(\alpha_2 - \dot{H}_2 \dot{\boldsymbol{q}}_2\Big) \end{bmatrix} + N_h + J_h^\top \boldsymbol{w} + \begin{bmatrix} J_1^\top R_1 \hat{\boldsymbol{z}} \beta \\ 0 \end{bmatrix}$$

where $\alpha_i = \ddot{\boldsymbol{s}}_{iv,d} + K_{f,d}\dot{\boldsymbol{s}}_{iv,e} + K_{f,p}\boldsymbol{s}_{iv,e}$ with $\boldsymbol{s}_{iv,d}$ be the desired value of $\boldsymbol{s}_{iv}$ and $\boldsymbol{s}_{iv,e} = \boldsymbol{s}_{iv,d} - \boldsymbol{s}_{iv}$, $\beta = w_e^b + K_{f,i}\int w_e^b \,\mathrm{d}t$ with w_e^b be the force error along the selected directions in the contact frame $\{F_{1d}\}$, and N_h is the nonlinear term calculated based on the arm controller output $\boldsymbol{\tau}_{a,\mathrm{ctrl}}$.

III. Power Grasp via Finger Gaits

In this section, we introduce a manipulation strategy that follows pivoting to achieve a power grasp, which allows it to resist external disturbance in any directions. The knife can be repositioned and reoriented by the arm and hand as desired.

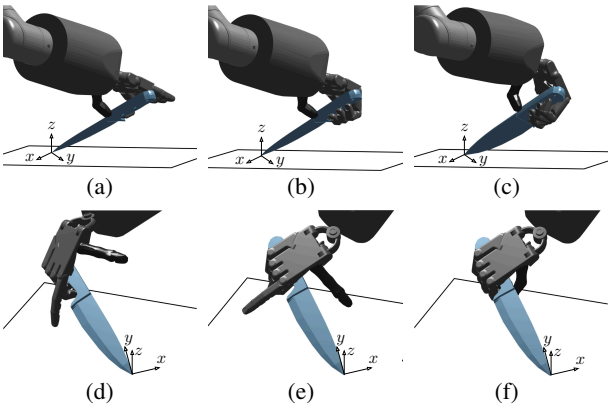

Fig. 4: Finger gaiting and hand caging to generate a power grasp. (a) End of pivoting; (b) wrapping around the knife's handle; (c) reorienting the hand and knife; (d) removing the thumb and index finger; (e) moving the palm towards the knife plane of symmetry; (f) closing in the thumb and index finger.

A. Wrapping Around Fingers

As shown in Fig. 4 (a), at time t_2 when pivoting ends, the knife's handle has been lifted up and in contact with the palm. From t_2 to time $t_3 > t_2$, the joints of each of the finger 3, 4, 5 close , in order to establish more contacts with the handle. A joint stops moving as soon as one of its descendent link collides with the handle, the joint reaches its limit, or it is constrained by other already fixed joints.

The knife is stabilized by the thumb and index finger at the antipodal positions on its handle. With the palm and the extra three fingers engaged in contact, there is little need for torsional torques at $\boldsymbol{p}_1$ and $\boldsymbol{p}_2$ to balance the knife's rotation along the antipodal line ℓ.[4] Any motion of the knife relative to the hand can be prevented.

B. Caging

Next, the thumb and the index finger will be relocated. They are first detached from the handle. During the action, the palm and the rest of the fingers need to prevent the knife from sliding out of the hand. The knife does not need to be completely caged due to assistance from the gravity and friction.

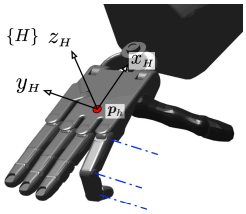

Fig. 5: Palm frame.

As shown in Fig. 5, the palm frame $\{H\}$ is situated at the palm's center of mass $\boldsymbol{p}_h$ with its y_H-axis aligned with the finger's common joint axis direction when all the joint angles are zero, and z_H-axis perpendicular to the palm inner plane and pointing outward from back of the palm. Denote by ξ the angle between the vector $\boldsymbol{p}_h - \boldsymbol{p}_0$ and the table plane. For a general knife handle shape, all the contact forces should stay inside their friction cone if $\xi < \tan^{-1}\mu$. To achieve such configuration, from time t_3 to some time $t_4 > t_3$, the hand rotates about the y_W-axis of the world frame $\{W\}$ with a certain angle such that the corresponding rotation matrix R_c satisfies the following constraint:

$$\tan\xi(t_4) = \frac{\hat{\boldsymbol{z}}^\top R_c\, \boldsymbol{p}_p(t_3)}{\|\boldsymbol{p}_p(t_3) - \hat{\boldsymbol{z}}\hat{\boldsymbol{z}}^\top R_c\, \boldsymbol{p}_p(t_3)\|} < \mu$$

.

Since the motion of the knife in other directions is either constrained by the palm and fingers geometrically or prevented by gravity (conservation of the energy), we see that without changing the finger tip position, the knife cannot escape from the hand. We refer readers to [7] for a through study of caging.

C. Power Grasp

As shown in Fig. 4(d), the finger 1 and 2 are removed after the 'caging' configuration, during time $[t_4, t_5]$.

Let rotation matrix R_h represent the orientation of the palm frame $\{H\}$ and $\boldsymbol{p}_5$ be the center of mass of the little finger's distal link. From time t_5 to $t_6 > t_5$, the palm is reoriented around $\boldsymbol{p}_5$ to achieve a final orientation $R_h(t_6) = R(t_2)$, which is aligned with the knife frame $\{B\}$. The palm trajectory is then represented as $R_h(t)$ and $\boldsymbol{p}_h(t) = R_h(t)\,{}^H\boldsymbol{p}_5(t_4)$, $t \in (t_5, t_6)$,

[4]Exertion of a large amount of such torque could also exceed the joint actuator limit.

where ${}^{H}\boldsymbol{p}_5(t_4) = R_h(t_4)^\top[\boldsymbol{p}_5(t_4) - \boldsymbol{p}_h(t_4)]$ is the position of little finger tip center relative to the palm frame $\{H\}$ at time t_4. In the meantime, the finger 3, 4, 5 have their tip positions maintained while joint angles changing passively to accommodate the palm motion. It is depicted in Fig. 4(d)–(e). Finally, the thumb and the index finger wrap around the the knife's handle along some predefined trajectory for the hand to achieve a power grasp configuration (Fig. 4(f)).

IV. Discussion

The presented strategy for gripping a resting kitchen knife is inspired by the action of a human hand, which naturally minimizes the effort (by leveraging the cutting board's support) and swiftly applies finger gaits to reach a power grasp on the knife's handle. While raising the handle, the human hand often eases effort by allowing the tip to slide a little on the cutting board, and then rotates the handle within the hand through a complex finger movement. All the intricacies of the human hand movements that comprise this single skill are at present beyond full replication or automation by the robot, because the human hand has different kinematics, superior tactile sensing capability, and unmatched skin elasticity. Nevertheless, close interleaving of continuous control policies and discrete topological transitions is a promising path to human-level dexterity.

Only simulation has been conducted due to the unavailability of an anthropomorphic hand in our lab. The right-hand model of the Shadow Hand E-Series and the UR10 arm are used in the simulation to manipulate a variety of knives in different scenarios.[5] A 6-axis force/torque sensor is mounted between the arm and hand. All simulations are performed with the MuJoCo physics engine [14].[6] All the plots shown in the paper and the accompanying video are generated by controllers running at the frequency of 500Hz.

The introduced gripping strategy can be carried out with any hand-arm pair that have considerably fewer number of DOFs. Since the hand has the freedom to rotate along the antipodal line, only five DOFs are required for the arm. The initial antipodal grasp requires the thumb and index finger to have at least three DOFs, while achievement of the power grasp requires each of the remaining fingers to have at least two DOFs.

Our strategy has overlooked several issues: slipping at the knife's tip, knife stabilization against horizontal swaying, etc. For finer finger gaits, we also need to consider kinematics of contact [15] between the fingertips and the handle, and incorporate them into the system dynamics and controller design as in [16]. We can consider impedance control for stabilizing the knife while it is being raised and grasped [17].

[5]The mass densities of the knife's blade and handle are set to be 8000 $\mathrm{kg/m^3}$ and 600 $\mathrm{kg/m^3}$. Coefficients of friction range from 0.5 to 2 for the knife-finger contact and from 0 to 0.1 for the knife-board contact. The torsional torque coefficient ranges from 0.005 to 0.05.

[6]The soft finger contact is modeled as a pyramidal friction cone coupled with a torsional torque opposing any rotation around the contact normal. Couplings among finger joints are described by equality constraints over their angles. The time step of simulation is set to be 2ms. The controller gain parameters are all diagonal matrices $K_{a,p}, K_{a,d}, K_{a,i}, K_{f,p}, K_{f,d}, K_{f,i}$ with the same entries 1000, 20, 20, 500, 100, 20, on their diagonals, respectively.

References

[1] H. Hoffmann, Z. Chen, D. Earl, D. Mitchell, B. Salemi, and J. Sinaopv. Adaptive robotic tool use under variable grasps. *Robotics and Autonomous Systems*, 62:833–846, 2014.

[2] J. Stückler and S. Behnke. Adaptive tool-use strategies for anthropomorphic service robots. In *IEEE/RAS Int. Conf. on Humanoid Robots*, pages 755–760, 2014.

[3] T. Hasegawa, T. Suehiro, and K. Takase. A model-based manipulation system with skill-based execution. *IEEE Trans. Robot. Autom.*, 8(5):535–544, 1992.

[4] J. Nakanishi, R. Cory, M. Mistry, J. Peters, and S. Schaal. Operational space control: A theoretical and empirical comparison. *Int. J. Robot. Res.*, 27(6):737–757, 2008.

[5] Jean J Moreau. Unilateral contact and dry friction in finite freedom dynamics. In *Nonsmooth mechanics and Applications*, pages 1–82. Springer, 1988.

[6] J. Hong, G. Lafferriere, B. Mishra, and X. Tan. Fine manipulation with multifinger hands. In *Proc. IEEE Int. Conf. Robot. Autom.*, pages 1568–1573, 1990.

[7] A. Rodriguez, M. T. Mason, and S. Ferry. From caging to grasping. *Int. J. Robot. Res.*, 31(7):886–900, 2012.

[8] Y. Yu, K. Takeuchi, and T. Yoshikawa. Optimization of robot hand power grasps. In *Proc. IEEE Int. Conf. Robot. Autom.*, volume 4, pages 3341–3347. IEEE, 1998.

[9] A. Holladay, R. Paolini, and M. T. Mason. A general framework for open-loop pivoting. In *Proc. IEEE Int. Conf. Robot. Autom.*, pages 3675–3681. IEEE, 2015.

[10] Y. Hou, Z. Jia, A. M. Johnson, and M. T. Mason. Robust planar dynamic pivoting by regulating inertial and grip forces. In *Workshop on the Algorithmic Foundations of Robotics*, 2016.

[11] N. C. Dafle, A. Rodriguez, R. Paolini, B. Tang, S. S. Srinivasa, M. Erdmann, M. T Mason, I. Lundberg, H. Staab, and T. Fuhlbrigge. Extrinsic dexterity: In-hand manipulation with external forces. In *Proc. IEEE Int. Conf. Robot. Autom.*, pages 1578–1585, 2014.

[12] Y.-B. Jia. Computation on parametric curves with application in grasping. *Int. J. Robot. Res.*, 23(7):825–855, 2004.

[13] R. M. Murray, Z. Li, and S. S. Sastry. *A Mathematical Introduction to Robotic Manipulation*. CRC Press, 1994.

[14] E. Todorov. Convex and analytically-invertible dynamics with contacts and constraints: Theory and implementation in mujoco. In *IEEE Int. Conf. Robot. Autom.*, pages 6054–6061, 2014.

[15] D. J. Montana. The kinematics of contact and grasp. *Int. J. Robot. Res.*, 7(3):17–32, 1988.

[16] A. Cole, J. Hauser, and S. Sastry. Kinematics and control of multifingered hands with rolling contact. In *Proc. IEEE Int. Conf. Robot. Autom.*, pages 228–233, 1988.

[17] V. R. Garate, M. Pozzi, D. Prattichizzo, N. Tsagarakis, and A. Ajoudani. Grasp stiffness control in robotic hands through coordinated optimization of pose and joint stiffness. *IEEE Robotics and Automation Letters*, 3(4):3952–3959, 2018.